# Formation of nonmagnetic $c$-$Fe_{1-x}Si$ in antiferromagnetically coupled epitaxial Fe/Si/Fe

G. J. Strijkers,* J. T. Kohlhepp, H. J. M. Swagten, and W. J. M. de Jonge
*Department of Physics and COBRA, Eindhoven University of Technology, P.O. Box 513, 5600 MB Eindhoven, The Netherlands*
(Received 29 March 1999)

Low-energy electron diffraction, Auger electron spectroscopy, and conversion electron Mössbauer spectroscopy have been applied to study antiferromagnetically exchange-coupled epitaxial Fe/Si/Fe(100). It is shown that a bcc-like (100) structure is maintained throughout the layers after a recrystallization of the spacer layer by Fe/Si interdiffusion. Direct experimental evidence is presented that $c$-$Fe_{1-x}Si$ ($0 \leqslant x \leqslant 0.5$) is formed in the spacer layer, a nonmagnetic metallic metastable iron silicide phase with a CsCl structure ($B2$), which supports explanations for the antiferromagnetic exchange coupling given recently. [S0163-1829(99)02837-4]

Since the discovery of strong antiferromagnetic (AF) interlayer coupling in Fe/Si multilayers[1] there have been a number of studies addressing the transformation of the Si spacer layer into iron silicide and its relation to the observed interlayer coupling. It is now well established that a metallic iron silicide formed by Fe/Si interdiffusion is responsible for the interlayer coupling.[2–9] The exact composition of the iron silicides in the spacer layer is considered to be crucial to understanding the exponential decay of the AF coupling with the interlayer thickness[8] in the framework of the Anderson $sd$-mixing model[10] or the electron-optics model.[11] In several studies[2,7,9] it is suggested that Fe and Si form an FeSi alloy spacer layer with a metastable CsCl structure ($c$-FeSi) and an Fe:Si ratio close to 1. Although it has been shown that $c$-FeSi can be stabilized epitaxially,[12,13] the spontaneous formation of $c$-FeSi in antiferromagnetically coupled Fe/Si-based layers has not been directly observed up to now to our knowledge. In this paper we present direct experimental evidence for the presence of $c$-$Fe_{1-x}Si$ with $0 \leqslant x \leqslant 0.5$ in the spacer layer of AF coupled Fe/Si/Fe by means of low-energy electron diffraction (LEED), Auger electron spectroscopy (AES), and conversion electron Mössbauer spectroscopy (CEMS).

Fe/Si/Fe layers were grown in a molecular-beam epitaxy (MBE) system (VG-Semicon V80M) with a base pressure of $2 \times 10^{-11}$ mbar. An $e$-gun source with feedback control of the flux was used for the deposition of natural Fe, whereas $^{56}Fe$, $^{57}Fe$, and Si were evaporated from temperature-stabilized Knudsen cells. All thicknesses were controlled by calibrated quartz-crystal monitors. The layers were grown at room temperature on Ge(100) substrates, which were cleaned by several $Ar^+$ sputter (700 °C) and anneal (780 °C) treatments until a sharp Ge(100)-($2 \times 1$) LEED pattern and no more C and O contaminations were observed. The LEED and AES measurements were performed *in situ* during several stages of the Fe and Si growth utilizing wedge-shaped as well as homogeneous layers. The room-temperature CEMS measurements were done *ex situ* in a spectrometer with a $^{57}CoRh$ source and a gas-flow detector.

Figure 1 shows the LEED patterns at 171 eV and LEED $I$-$V$ curves of the 00 spot during several stages of the growth of Ge(100)+60 Å Fe+12 Å Si+45 Å Fe. The penetration depth of the electrons at this energy is typically 3–4 ML, which ensures that we mainly probe the surface layers. After deposition of the 60 Å Fe layer, a ($1 \times 1$) LEED pattern of a bcc-Fe(100) surface is observed with relatively sharp spots, indicating good single-crystalline growth of the Fe on the Ge(100) substrate. The good crystallinity was further confirmed by magneto-optical Kerr effect (MOKE) measurements that showed hard and easy axes of magnetization for fields applied along the [100] and [110] directions, respectively, as expected for single-crystalline bcc-Fe. LEED patterns (b), (c), and (d) show that upon deposition of Si the spots become more and more faint and completely disappear between 8 and 9 Å. For 12 Å Si only a bright background is left, which means that Si grows, at least above 9 Å, in an amorphous or at least strongly disordered manner onto the Fe.

When Fe is deposited on this disordered 12 Å Si layer, the sharp ($1 \times 1$) LEED pattern with the spots at exactly the same position reappears again at a nominal layer thickness of about 5 Å Fe, as shown in patterns (e) and (f). This implicates that by diffusion of Fe into the spacer a recrystallization of the disordered Si has taken place into crystalline iron silicide. If this would not be the case one would expect poly-

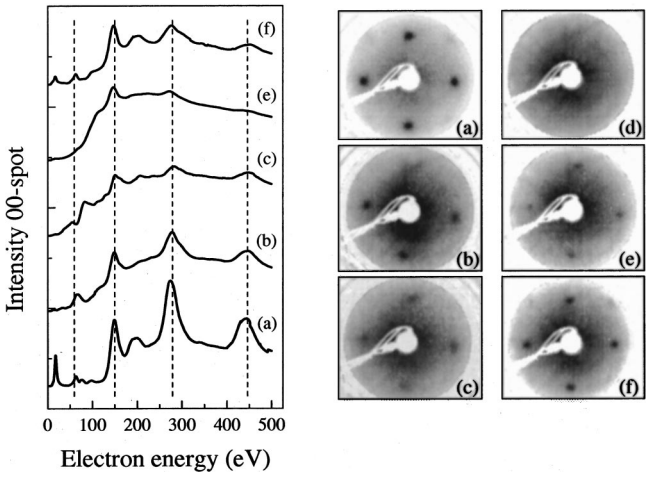


FIG. 1. (left panel) LEED $I$-$V$ curves of the 00-spot intensity (no background correction) and (right panel) LEED patterns at 171 eV of Ge(100) + (a) 60 Å Fe, (b) 60 Å Fe+6 Å Si, (c) 60 Å Fe+8.5 Å Si, (d) 60 Å Fe+12 Å Si, (e) 60 Å Fe+12 Å Si+6 Å Fe, (f) 60 Å Fe+12 Å Si+45 Å Fe.

 

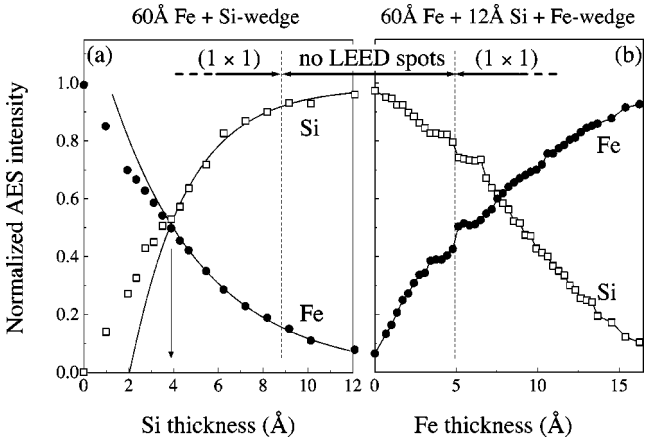


FIG. 2. Normalized Si 92-eV *LVV* (open squares) and Fe 47-eV *MVV* (solid circles); AES peak intensities versus the nominal Si and Fe layer thickness for the growth of (a) Si on 60 Å Fe and (b) Fe on 60 Å Fe+12 Å Si, respectively. The solid lines in (a) are exponential fits to the data for $t_{Si} \geq 4$ Å .

crystalline rather than single-crystalline growth of the top Fe layer. This reappearance of the LEED pattern can be observed up to a 21 Å Si spacer but disappears for larger thicknesses, indicating a limited diffusion depth at room temperature. A Fe/Si-wedge/Fe trilayer prepared in this way shows strong antiferromagnetic interlayer exchange coupling, whose strength varies exponentially with the nominal Si layer thickness[14] in accordance with de Vries *et al.*[8] for layers grown at 200 °C.

In the left panel of Fig. 1 the 00-spot intensity versus the electron energy is plotted corresponding to the LEED pattern at the right-hand side, except for (d) in which no LEED spots were found. Upon deposition of Si the *I-V* curves become less structured, but regain better pronounced peaks after deposition of the top Fe layer. Additionally, from the positions of the main Bragg reflections, as indicated with dashed lines in Fig. 1, it can be concluded that the perpendicular lattice constant remains constant at $\approx 1.43$ Å close to bulk values for Fe ($d_{100} = 1.4331$ Å). Thus, a bcc-like (100) growth is maintained throughout the whole structure.

To obtain more insight in the iron silicide formation process we followed the growth of a Si wedge on Fe and an Fe wedge on Si by AES. In Fig. 2(a) the evolution of the Auger Si *LVV* (92-eV) and Fe *MVV* (47-eV) peak intensities are plotted as a function of the nominal Si thickness deposited on a single crystalline 60 Å Fe base layer. For a Si coverage of about 4 Å a change of slope is observed in both Fe and Si intensities, a clear sign of interdiffusion between the bottom Fe and the top Si layer up to this thickness, in agreement with earlier observations by Gallego and Miranda.[15] For coverages above 4 Å the AES intensities can be described with exponentials (solid lines in the figure) with attenuation lengths in agreement with closed Si-layer growth, excluding further intermixing.

In Fig. 2(b) the evolution of the Si and Fe Auger intensities are presented for an Fe wedge deposited on 60 Å Fe+12 Å Si. A jump and two adjacent plateaus in the Fe as well as in the Si AES intensities are observed between 3.5 and 6.5 Å nominal Fe thickness. The jump at an Fe thickness of about 5 Å is accompanied by the already mentioned reappearance of the $(1 \times 1)$ LEED pattern. Apparently, at this point a recrystallization of the spacer layer takes place. The plateaus can be understood assuming that an equilibrium is reached between Fe deposition on top of the spacer layer and Fe diffusion into the spacer layer. When the Si spacer is saturated with Fe above 6.5 Å, an exponential increase and decrease of Fe and Si AES intensities, respectively, is observed, indicating a closed layer growth of Fe. The Fe and Si intensity ratios at the plateaus $I_{Fe}/I_{Si} = 0.56$ and 0.83, calculated from the absolute intensities, indicate that $Fe_{1-x}Si$ is formed with $x$ in the range from 0 to 0.5, according to Gallego and Miranda.[15] However, we have to realize that the interdiffusion of Fe with Si is a complex process and Fe or Si segregation at the surface and the observed recrystallization can seriously alter the AES intensity ratio. Therefore, a definite identification of the formed iron silicide phases cannot be given from the AES intensities alone.

The high sensitivity of CEMS to the local atomic environment together with the well-known Mössbauer parameters for the relevant iron silicides gives us the opportunity to identify the iron silicides formed in our exchange-coupled layers. Furthermore, position sensitive identification of the iron silicides can be obtained using a $^{57}$Fe probe layer that easily can be shifted through the multilayer stack.

The measurements were performed on separately grown samples with 6 Å $^{57}$Fe probe layers at various positions in an $^{56}$Fe matrix, guaranteeing that the Fe in the iron silicide of the spacer layer can be clearly discriminated from the rest of the Fe, in contrast to earlier studies.[2,16,9] A first sample was designed to give information about the iron silicide spacer layer only, with the following nominal composition: Ge(100)+68 Å $^{56}$Fe+3×(16 Å Si+6 Å $^{57}$Fe+19 Å $^{56}$Fe) +30 Å Si, schematically sketched in the inset of Fig. 4. The relatively thick $^{56}$Fe buffer layer prevents that any iron germanide formation distorts the CEMS data and three repetitions were chosen for sensitivity reasons. For a nominally 16 Å-thick Si spacer layer, AES measurements established that 6 Å $^{57}$Fe will completely react with the Si, ensuring that the observed CEMS spectrum is only due to the nonmagnetic iron silicide in the spacer responsible for the interlayer exchange coupling. We will refer to this sample as ''reference'' in the following. A second series was grown with the nominal composition: Ge(100)+60 Å Fe+3×(10 Å Si+31 Å Fe)+30 Å Si, with the 6 Å $^{57}$Fe probe layers deposited 4 Å below, 2 Å below, at the bottom of, on top of, and 6 Å above the Si spacer, as schematically sketched in Fig. 5.

Figure 3 shows the MOKE hysteresis loops for the 16 Å-thick spacer, and for one sample of the second series with 10 Å nominal spacer thickness. Both loops show evidence of AF coupling with clear plateaus and high saturation fields. The high remanence is mainly caused by the thick Fe buffer layer. We want to emphasize that for all of the samples, for which the CEMS results will be presented in the following, AF coupling is present, a necessary condition because we want to investigate the iron silicide responsible for the coupling.

The CEMS spectrum of the reference sample is presented in Fig. 4. The spectrum consists of one quadrupole splitted line, which can be fitted well with a distribution of quadrupole doublets. The fitting parameters, isomer shift ($\delta$), and quadrupole splitting ($\Delta$) in the maximum of the distribution

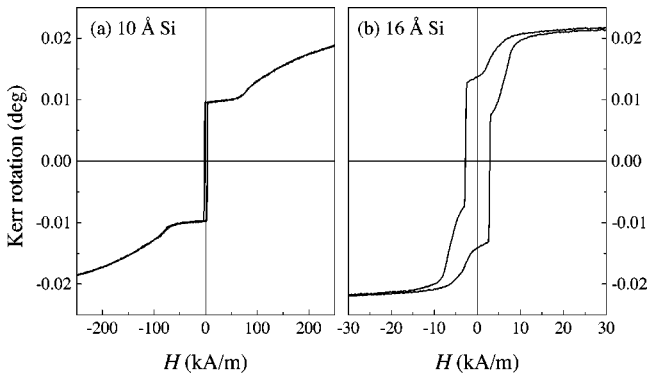


FIG. 3. Representative longitudinal Kerr hysteresis loops of the Fe/Si samples with $^{57}Fe$ probe layers and nominal spacer layer thickness of (a) 10 Å Si and (b) 16 Å Si, respectively. The field is applied along the [100] directions of the samples (easy axis of the Fe layers).

are listed in Table I. There are several possible iron silicides reported in the literature[12,13] that qualify for the observed apparently nonmagnetic iron silicide.

The first one is $\epsilon$-FeSi, a nonmagnetic small-gap semiconductor with a cubic symmetry (B20). The local Fe symmetry is, however, trigonal, which results in a quadrupole splitted CEMS spectrum with $\delta = 0.26$ mm/s and $\Delta = 0.51$ mm/s, close to what we observe.[17] However, the formation of an $\epsilon$-FeSi spacer is impossible because our LEED results clearly show that an epitaxial relationship is maintained throughout the whole stack of layers, incompatible with the lattice parameters of $\epsilon$-FeSi. Furthermore, no semiconducting properties of the spacer layer were found from the temperature dependence of the interlayer coupling.[14]

A second candidate is $\alpha$-$FeSi_2$, the metallic state of iron disilicide with a tetragonal structure and with Mössbauer parameters $\delta = 0.23$ mm/s and $\Delta = 0.47$ mm/s for one doublet and $\delta = 0.26$ mm/s and $\Delta = 0.73$ mm/s for a second doublet.[17] Although the parameters of the first doublet match perfectly with our results, we do not observe a second maximum in the distribution matching the second known doublet

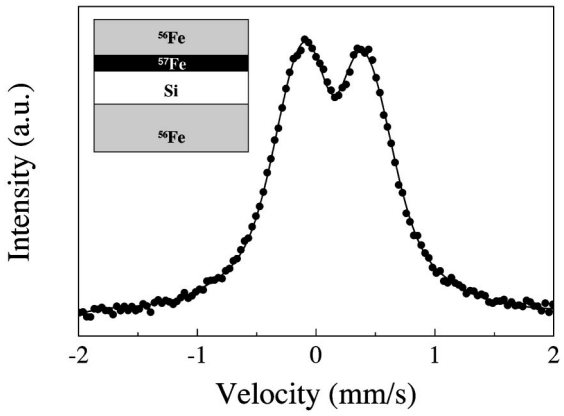


FIG. 4. CEMS spectrum of Ge(100)+68 Å $^{56}Fe$+3×(16 Å Si+6 Å $^{57}Fe$+19 Å $^{56}Fe$)+30 Å Si. $^{57}Fe$ deposited directly onto the Si will diffuse completely into the spacer, ensuring that the spectrum is only caused by Fe in the formed iron silicide spacer. The solid line is a fit with a distribution of quadrupole splitted doublets.

TABLE I. Isomer shift ($\delta$), quadrupole splitting ($\Delta$), hyperfine field ($B_{hf}$), and relative intensities ($I_d$, and $I_s$) of doublets and sextets as obtained from fits to the experimental CEMS spectra. Isomer shifts are given relative to $\alpha$-Fe.

| | Doublet | | | Sextet | | |
|---|---|---|---|---|---|---|
| $^{57}Fe$ position | $\delta$ (mm/s) | $\Delta$ (mm/s) | $I_d$ (%) | $\delta$ (mm/s) | $B_{hf}$ (T) | $I_s$ (%) |
| Reference | 0.24 | 0.47 | 100 | | | |
| 6 Å above | | | | 0.012 | 32.4 | 100 |
| On top of Si | 0.24 | 0.43 | 15 | 0.076 | 28.0 | 85 |
| Below Si | 0.24 | 0.43 | 29 | 0.059 | 29.4 | 71 |
| 2 Å below Si | 0.24 | 0.43 | 17 | 0.037 | 31.6 | 83 |
| 4 Å below Si | | | | 0.009 | 32.9 | 100 |

parameters. Furthermore, the perpendicular lattice constant is inconsistent with our LEED results.

The remaining candidate is nonmagnetic $c$-$Fe_{1-x}Si$, a metallic metastable phase with a CsCl structure ($B2$). Stoichometric $c$-FeSi has an isomer shift of $\delta = 0.26$ mm/s, but no quadrupole splitting due to its cubic symmetry.[12,13] However, when Fe vacancies are introduced ($c$-$Fe_{1-x}Si$) a quadrupole splitting is observed consistent with our results. For example, Fig. 4 shows a remarkable resemblance with the slightly assymetric quadrupole splitted doublet of $c$-$Fe_{0.5}Si$ as reported by Fanciulli *et al.*[12] In their study the spectrum was fitted with three quadrupole splitted doublets, associated to different Fe sites of which the doublet with the highest intensity has a quadrupole splitting of $\Delta = 0.47$ mm/s, in agreement with our data. Furthermore, we have to realize that also strain reduces the local cubic symmetry introducing an electric field gradient. Thus we might already expect a quadrupole splitting for stoichometric $c$-FeSi grown coherently on bcc-Fe. From the previous analysis we conclude that our spacer layer exists of, possibly strained, nonstoichometric silicon rich $c$-FeSi with a CsCl structure.

Additional information can be gained from the second series of samples in which the $^{57}Fe$ probe layer is shifted through the stack from nominally 4 Å below to 6 Å above the spacer layer. Figure 5 shows the CEMS spectra for the different positions. It is clear from the raw data already that the $^{57}Fe$ spectra far enough from the spacer are identical and consist of a magnetically splitted Fe sextet, whereas the other spectra are a mixture of magnetic Fe from the magnetic layers and the nonmagnetic $c$-$Fe_{1-x}Si$ doublet from the spacer layer. All the spectra are fitted with a distribution of hyperfine fields and, if present, a distribution of quadrupole splittings for the nonmagnetic doublet. The relative intensity ratio of the sextets is 3:4:1:1:4:3 for all spectra indicating an in-plane magnetization direction in agreement with our magnetization measurements. The resulting Mössbauer parameters in the maximum of the distributions are listed in Table I.

The hyperfine field of the magnetically splitted part of the spectrum can be related to magnetic iron silicide alloys using previous work by Stearns.[18] The maximum of the hyperfine field ranges from 32.9 T, close to pure $\alpha$-Fe for the probe layer at 4 Å below the Si, to 28.0 T, which can be assigned to $Fe_{82}Si_{18}$ for the probe layer directly on top of the Si. For all positions there is a broad distribution in hyperfine fields, indicating that there is a composition gradient from pure Fe

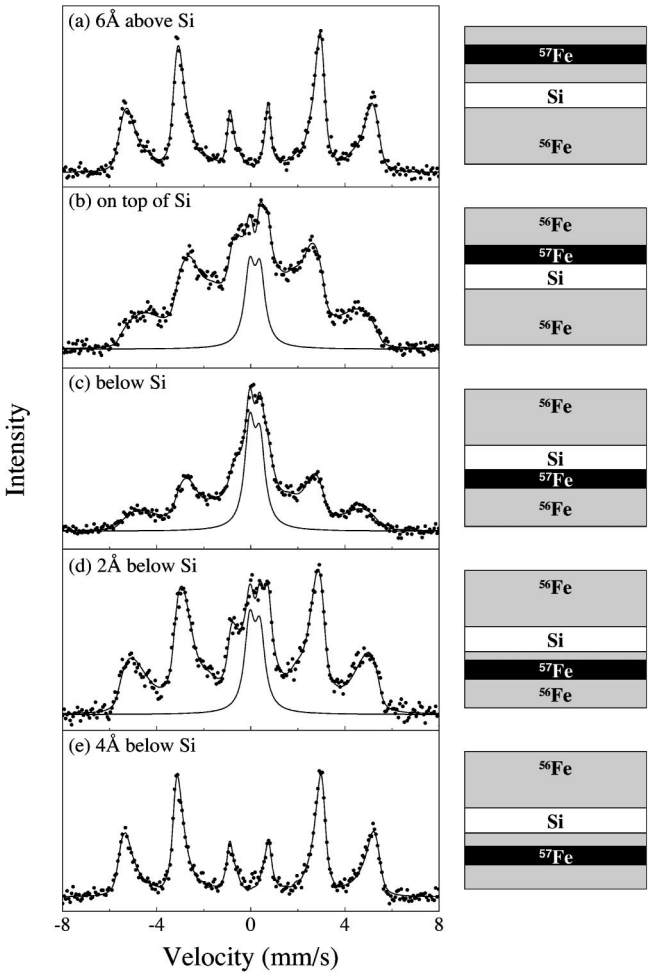


FIG. 5. CEMS spectra of Ge(100)+60 Å Fe+3×(10 Å Si+31 Å Fe)+30 Å Si with a 6 Å $^{57}$Fe probe layer deposited at various positions in the multilayer stack as indicated in the figure. The solid lines are fits to the experimental spectra as explained in the text.

in the bulk of the magnetic layers towards $c$-$Fe_{1-x}Si$ in the spacer layer. Furthermore, an asymmetric iron silicide profile is observed in spectra (b) and (c). More Fe diffuses from the bottom than from the top into this 10 Å Si layer. It is clear that the Fe/Si and Si/Fe interface are inequivalent with respect to the iron silicide formation, an observation earlier made by photoemission studies by Kläsges *et al.*[19]

The same $c$-$Fe_{1-x}Si$ doublet as for the reference sample is found in spectra (b), (c), and (d), although the quadrupole splitting is slightly lower, which could be a sign of more stoichometric $c$-FeSi. A thickness-dependent strain effect, however, would result in an increased quadrupole splitting for thinner layers instead of the decrease observed.[13] The $c$-$Fe_{1-x}Si$ doublet is found not only for the probe layer directly below and on top of the Si layer but also for 2 Å below, which confirms the AES results that Fe diffuses also from the bottom into the Si. From the total intensities of the doublets and sextets we estimate that between 3 and 3.3 Å $^{57}$Fe and about 8 Å Si contribute to the nonmagnetic doublet, which results in $c$-$Fe_{1-x}Si$ with an average $x$ in the range between 0.30 and 0.36, using bulk mole volumes of Fe and Si.

One might argue that the complex formation of $c$-$Fe_{1-x}Si$ by diffusion of Fe into the Si spacer layer could strongly depend on the preparation methods and conditions, which might make a universal interpretation of the interlayer exchange coupling in Fe/Si-based layers impossible. However, as was already shown before,[8,9] the thickness dependence and strength of the coupling are generally the same for layers prepared with initially different FeSi spacer and magnetic layer compositions. Apparently, the interlayer exchange coupling does not depend crucially on the exact spacer layer composition, as long as a crystalline FeSi spacer is formed with the CsCl structure. This is confirmed by recent calculations by Moroni *et al.*,[20] who have shown that the density of states near the Fermi level for stoichometric and defective $c$-FeSi are almost identical, including a sharp peak in the density of states about 0.2 eV above the Fermi level. Within the framework of the Anderson $sd$-mixing model, this peak is believed to mediate the coupling in Fe/Si-based layers.

In conclusion we have systematically studied iron silicide formation in AF coupled Fe/Si/Fe(100) layers. With LEED and AES it was confirmed that a crystalline iron silicide is formed in the spacer layer, which was identified as $c$-$Fe_{1-x}Si$ from CEMS measurements. The formation of $c$-FeSi corroborates recent explanations for the observed antiferromagnetic exchange coupling in Fe/Si based layers.[8]

The work of G.J.S. was supported by the Foundation for Fundamental Research on Matter (FOM).

*Author to whom correspondence should be addressed; electronic address: Strijkers@phys.tue.nl

[1] E. E. Fullerton, J. E. Mattson, S. R. Lee, C. H. Sowers, Y. Y. Huang, G. Felcher, and S. D. Bader, J. Magn. Magn. Mater. **117**, L301 (1992).

[2] E. E. Fullerton, J. E. Mattson, S. R. Lee, C. H. Sowers, Y. Y. Huang, G. Felcher, S. D. Bader, and F. T. Parker, J. Appl. Phys. **73**, 6335 (1993).

[3] C. L. Foiles, M. R. Franklin, and R. Loloee, Phys. Rev. B **50**, 16 070 (1994).

[4] J. Dekoster, A. Vantomme, S. Degroote, R. Moons, and G. Langouche, in *Structure and Properties of Multilayered Thin Films*, edited by T. D. Nguyen *et al.*, MRS Symposia Proceedings No. 382 (Materials Research Society, Pittsburgh, 1995), p. 253.

[5] A. Chaiken, R. P. Michel, and C. T. Wang, J. Appl. Phys. **79**, 4772 (1996).

[6] J. A. Carlisle, A. Chaiken, R. P. Michel, L. J. Terminello, J. J. Jia, T. A. Callcott, and D. L. Ederer, Phys. Rev. B **53**, R8824 (1996).

[7] A. Chaiken, R. P. Michel, and M. A. Wall, Phys. Rev. B **53**, 5518 (1996).

[8] J. J. de Vries, J. Kohlhepp, F. J. A. den Broeder, R. Coehoorn, R. Jungblut, A. Reinders, and W. J. M. de Jonge, Phys. Rev. Lett. **78**, 3023 (1997).

[9] J. T. Kohlhepp, J. J. de Vries, F. J. A. den Broeder, R. Coehoorn, R. M. Jungblut, A. Reinders, G. J. Strijkers, A. A. Smits, and W. J. M. de Jonge, in *Magnetic Ultrathin Films, Multilayer and Surfaces–1997*, edited by J. Tobin *et al.*, MRS Symposia Proceedings No. 475 (Materials Research Society, Pittsburgh, 1997), p. 593.

[10] Z.-P. Shi, P. M. Levy, and J. L. Fry, Europhys. Lett. **26**, 473 (1994).
[11] P. Bruno, Phys. Rev. B **52**, 411 (1995).
[12] M. Fanciulli, G. Weyer, H. von Känel, and N. Onda, Phys. Scr. **T54**, 16 (1994).
[13] M. Fanciulli, G. Weyer, A. Svane, N. E. Christensen, H. von Känel, E. Müller, N. Onda, L. Miglio, F. Tavazza, and M. Celino, Phys. Rev. B **59**, 3675 (1999).
[14] G. J. Strijkers, J. T. Kohlhepp, H. J. M. Swagten, and W. J. M. de Jonge (unpublished).
[15] J. M. Gallego and R. Miranda, J. Appl. Phys. **69**, 1377 (1991).
[16] J. Dekoster, H. Bemelmans, S. Degroote, R. Moons, J. Verheyden, A. Vantomme, and G. Langouche, J. Appl. Phys. **81**, 5349 (1997).
[17] Ö. Helgason and T. I. Sifüsson, Hyperfine Interact. **45**, 415 (1989).
[18] M. B. Stearns, Phys. Rev. **129**, 1136 (1963).
[19] R. Kläsges, C. Carbone, W. Eberhardt, C. Pampuch, O. Radar, T. Kachel, and W. Gudat, Phys. Rev. B **56**, 10 801 (1997).
[20] E. G. Moroni, W. Wolf, J. Hafner, and R. Podloucky, Phys. Rev. B **59**, 12 860 (1999).